Deep Learning Model of Diastolic Dysfunction Risk Stratifies the Progression of Early-Stage Aortic Stenosis

Running title: **Diastolic Dysfunction Predicts the Progression of Early-Stage Aortic Stenosis**

Márton Tokodi, MD, PhD[1,2]

Rohan Shah, MD[3]

Ankush Jamthikar, MTech, PhD[1]

Neil Craig, MD[4]

Yasmin Hamirani, MD[1]

Grace Casaclang-Verzosa, MD, MBA[1]

Rebecca T. Hahn, MD[5,6]

Marc R. Dweck, MD, PhD[4]

Philippe Pibarot, DVM, PhD[7]

Naveena Yanamala, MSc, PhD[1,8]

Partho P. Sengupta, MD, DM[1]

[1]Division of Cardiovascular Diseases and Hypertension, Rutgers Robert Wood Johnson Medical School, New Brunswick, NJ, USA

[2]Heart and Vascular Center, Semmelweis University, Budapest, Hungary

[3]Division of General Internal Medicine, Rutgers Robert Wood Johnson Medical School, New Brunswick, NJ, USA

[4]Centre for Cardiovascular Science, University of Edinburgh, Edinburgh, United Kingdom

[5]Department of Medicine, Columbia University Irving Medical Center, New York, NY, USA

[6]Cardiovascular Research Foundation, New York, New York, USA

[7]Québec Heart and Lung Institute, Department of Medicine, Laval University, Québec City, Québec, Canada

[8]Institute for Software Research, School of Computer Science, Carnegie Mellon University, Pittsburgh, PA, USA

CORRESPONDING AUTHOR

Partho P. Sengupta, MD, DM

Division of Cardiovascular Diseases and Hypertension

Rutgers Robert Wood Johnson Medical School

1 Robert Wood Johnson Place, New Brunswick, NJ 08901, USA

Phone: +1-732-828-3000

E-mail: partho.sengupta@rutgers.edu

WORD COUNT: 6,191 (text: 3,978; references: 1,605; figure legends: 608)

FUNDING

The work presented in this paper was supported in part by funds from the National Science Foundation (award number: 1920920). Dr. Tokodi was supported by the New National Excellence Program (ÚNKP-23-4-II-SE-39) of the Ministry of Culture and Innovation in Hungary from the National Research, Development, and Innovation Fund.

CONFLICT OF INTEREST

Dr. Tokodi has received consulting fees from CardioSight outside the submitted work. Dr. Hahn has received speaker fees from Abbott Structural, Baylis Medical, and Edwards Lifesciences; has institutional educational and consulting contracts for which she receives no direct compensation with Abbott Structural, Boston Scientific, Edwards Lifesciences, and Medtronic; and is the chief scientific officer for the Echocardiography Core Laboratory at the Cardiovascular Research Foundation for multiple industry-sponsored trials for which she receives no direct industry compensation. Dr. Dweck is supported by the British Heart Foundation (FS/14/78/31020) and has received the Sir Jules Thorn Award for Biomedical Research 2015 (15/JTA). He has received speaker fees from Pfizer, Radcliffe Cardiology, Bristol Myers Squibb, Edwards, and Novartis and consulting fees from Novartis, Jupiter Bioventures, Beren, and Silence Therapeutics. Dr. Pibarot has received funding from Edwards Lifesciences, Medtronic, Pi-Cardia, and Cardiac Success for echocardiography core laboratory analyses and research studies in transcatheter valve therapies, for which he received no personal compensation. Dr. Pibarot has also received lecture fees from Edwards Lifesciences and Medtronic. Dr. Yanamala serves as an advisor for Turnkey Techstart. Dr. Sengupta serves as an advisor for Echo IQ and RCE Technologies. All other authors have no conflict of interest to declare.

ABSTRACT

Background: The development and progression of aortic stenosis (AS) from aortic valve (AV) sclerosis is highly variable and difficult to predict.

Objectives: We investigated whether a previously validated echocardiography-based deep learning (DL) model assessing diastolic dysfunction (DD) could identify the latent risk associated with the development and progression of AS.

Methods: We evaluated 898 participants with AV sclerosis from the Atherosclerosis Risk in Communities (ARIC) cohort study and associated the DL-predicted probability of DD with two endpoints: (1) the new diagnosis of AS and (2) the composite of subsequent mortality or AV interventions. We performed validation in two additional cohorts: 1) patients with mild-to-moderate AS undergoing cardiac magnetic resonance (CMR) imaging and serial echocardiographic assessments (n=50), and (2) patients with AV sclerosis undergoing ^{18}F-sodium fluoride (^{18}F-NaF) and ^{18}F-fluorodeoxyglucose positron emission tomography (PET) combined with computed tomography (CT) to assess valvular inflammation and calcification (n=18).

Results: In the ARIC cohort, a higher DL-predicted probability of DD was associated with the development of AS (adjusted HR: 3.482 [2.061 – 5.884], p<0.001) and subsequent mortality or AV interventions (adjusted HR: 7.033 [3.036 – 16.290], p<0.001). The multivariable Cox model (incorporating the DL-predicted probability of DD) derived from the ARIC cohort efficiently predicted the progression of AS (C-index: 0.798 [0.648 – 0.948]) in the CMR cohort. Moreover, the predictions of this multivariable Cox model correlated positively with valvular ^{18}F-NaF mean standardized uptake values in the PET/CT cohort (r=0.62, p=0.008).

Conclusions: Assessment of DD using DL can stratify the latent risk associated with the progression of early-stage AS.

CONDENSED ABSTRACT

We investigated whether DD assessed using DL can predict the progression of early-stage AS. In 898 patients with AV sclerosis, the DL-predicted probability of DD was associated with the development of AS. The multivariable Cox model derived from these patients also predicted the progression of AS in an external cohort of patients with mild-to-moderate AS (n=50). Moreover, the predictions of this model correlated positively with PET/CT-derived valvular ^{18}F-NaF uptake in an additional cohort of patients with AV sclerosis (n=18). These findings suggest that assessing DD using DL can stratify the latent risk associated with the progression of early-stage AS.

KEYWORDS

aortic valve sclerosis, aortic stenosis, diastolic dysfunction, echocardiography, deep learning

ABBREVIATIONS

ARIC – Atherosclerosis Risk in Communities study

AS – aortic stenosis

AV – aortic valve

BioLINCC – Biologic Specimen and Data Repository Information Coordinating Center

CMR – cardiac magnetic resonance

CT – computed tomography

DD – diastolic dysfunction

DL – deep learning

ICD – International Classification of Diseases

LGE – late gadolinium enhancement

PET – positron emission tomography

SUV – standardized uptake value

Aortic valve (AV) sclerosis, defined as the calcification and thickening of the AV that does not cause significant obstruction in transvalvular flow, is a common finding, and its prevalence increases from 25% at the age of 65 to 50% at 80 (1,2). AV sclerosis progresses to aortic stenosis (AS) in 10-15% of patients over 5 years (3-5) and is associated with adverse outcomes, such as coronary events and cardiovascular as well as all-cause mortality (1,6). Accordingly, the American College of Cardiology (ACC) and the American Heart Association (AHA) have recommended defining AS during its early stages as AV sclerosis (Stage A) and mild-to-moderate AS (Stage B) (7).

Several factors, including age, hyperlipidemia, diabetes, smoking, and hypertension, influence the progression of AV sclerosis and other myocardial processes like left ventricular (LV) remodeling and systolic and diastolic dysfunction (DD) (2,8-10). Notably, among different myocardial changes, the alterations in diastolic function – an active, adenosine triphosphate-dependent process – occur early and may explain the association of subclinical DD with AV sclerosis, independent of the aforementioned cardiovascular risk factors (11). Additionally, the compromised myocardial energetics and mitochondrial dysfunction associated with AS also contribute to DD (12-14).

Given these complex associations, machine learning may aid in identifying subsets of patients with AV sclerosis who face an elevated risk of progressing to AS. Nonetheless, previous machine learning and deep learning (DL) studies have primarily focused on the diagnosis (15-17), prognostication (18), and follow-up of patients with AS (19). Saliency maps in recent electrocardiogram (ECG)-based DL models highlighted a strong dependence on the diastolic phase, specifically the end of the T and U waves, for detecting AS, along with the future risk of developing AS in those with no AS at baseline (20-23). Moreover, the probability of AS predicted by these ECG-based models correlated positively with several echocardiographic features that assess the overall severity of DD (21). Similarly, saliency maps

generated from a recent echocardiography-based DL model predicting the presence of AS from two-dimensional parasternal long-axis videos have demonstrated that the model also focused on other cardiac structures beyond the AV, and the model's predictions correlated with echocardiographic markers of elevated diastolic filling pressures, left atrial dilation, and elevated pulmonary pressures (24).

Accordingly, we hypothesized that a DL model that integrates multiple echocardiographic features for assessing DD could identify the latent risk associated with the progression of early-stage AS. First, we investigated the associations between DD assessed using a previously validated DL model and the development of AS in patients with AV sclerosis (Stage A) from a population-based cohort. Then, we also confirmed the relevance of the DL-predicted DD probabilities in predicting the progression of AS in a second cohort of patients with mild-to-moderate AS (Stage B). Last, to gain insights into the underlying biological pathways, we also correlated the DL-predicted DD probabilities with the extent of myocardial fibrosis quantified using cardiac magnetic resonance (CMR) imaging in the second cohort and, in a third cohort of patients, we also assessed valvular calcification and inflammation using ^{18}F-sodium fluoride (^{18}F-NaF) and ^{18}F-fluorodeoxyglucose (^{18}F-FDG) positron emission tomography (PET) combined with computed tomography (CT).

METHODS

Population-based cohort – the ARIC cohort

We investigated the development of AS from AV sclerosis (Stage A) using data collected at visit 5 in the Atherosclerosis Risk in Communities (ARIC) cohort study (25). We analyzed the data of those who underwent an echocardiographic examination at visit 5 between 2011 and 2013 and whose data was available in the Biologic Specimen and Data Repository Information Coordinating Center (BioLINCC) database (Figure 1). From the 5,576 participants who fulfilled these criteria, we excluded those with congenital heart disease (n=20), hypertrophic obstructive cardiomyopathy (n=1), previously diagnosed AS (n=193), previous AV interventions (n=46), a prosthetic valve at any position (n=47), moderate or severe aortic regurgitation (n=24), or moderate or severe mitral regurgitation (n=108). In addition, we also excluded participants with missing values in key echocardiographic variables (n= 282) or no follow-up data (n=3).

Echocardiographic protocol in the ARIC cohort

The echocardiographic protocol of visit 5 has been published previously (26) and is described briefly in the Supplemental Methods. AV sclerosis was defined as an AV peak velocity between 1.5 and 2.5 m/s (27). The presence and grade of DD were assessed based on the recommendations of the American Society of Echocardiography (ASE) and the European Association of Cardiovascular Imaging (EACVI) (28).

DL-based assessment of DD

We used our previously published and thoroughly validated DL model that assesses DD based on nine routinely measured echocardiographic parameters: LV ejection fraction [LVEF],

LV mass index [LVMi], left atrial volume index [LAVi], early mitral inflow velocity [E], late mitral inflow velocity (A), E/A, early diastolic mitral annular velocity at septal position [e'], E/e', and tricuspid regurgitation peak velocity (TRV) (29,30). The output of the DL model is a single numeric value for each subject, denoting the probability of DD. Further details on the DL model and its external validation are provided in the Supplemental Methods and have been previously published (30). The model is publicly available online (31).

Outcomes of interest in the ARIC cohort

The primary endpoint of our study was the new diagnosis of AS after visit 5, whereas the secondary endpoint was the composite of AV interventions and all-cause death after newly diagnosed AS. The time to event was measured from the date of the echocardiographic examination at visit 5. The new diagnosis of AS was established based on echocardiographic data available from abstracted hospitalizations or was defined as an event (hospitalization or death) with an International Classification of Diseases, 9th Revision (ICD-9) code of 424.1 or an ICD, 10th Revision (ICD-10) code of I35.0 or I35.2 in any position (Supplemental Table 1) (32). AV interventions were identified as hospitalizations with an ICD-9 procedure code of 35.01, 35.05, 35.06, 35.11, 35.21, 35.22, or 35.96 or an ICD-10 procedure code of 027Fx, 02NFx, 02QFx, or 02RFx in any position (Supplemental Table 2) (32). Participants not reaching these endpoints were followed up through December 31, 2018, date of death, or loss to follow-up, whichever occurred first.

Multimodality external validation cohorts

CMR cohort: We applied the DL model to the participants of the "The Role of Myocardial Fibrosis in Patients With Aortic Stenosis" prospective observational study (NCT01755936) (33). All subjects underwent detailed clinical evaluation at baseline, including

echocardiography and CMR imaging. Focal replacement fibrosis was assessed in all patients using late gadolinium enhancement (LGE), and diffuse fibrosis associated with extracellular volume expansion was assessed using myocardial T1 mapping. The details of the imaging protocol, image analysis, and validation against myocardial biopsy-derived histological myocardial fibrosis have been described previously (33). Patients were followed with annual echocardiographic examinations for two consecutive years. Progression of AS was defined as a worsening in the severity of AS (i.e., development of moderate or severe AS from mild or moderate AS, respectively). The severity of AS was determined based on AV mean gradient, AV peak velocity, AV area, and the dimensionless index.

PET/CT cohort: We also applied our DL model to the participants with AV sclerosis from the "Role of Active Valvular Calcification and Inflammation in Patients With Aortic Stenosis" observational cohort study (NCT01358513) (34). Participants in this study underwent echocardiography, non-contrast CT, and ^{18}F-NaF and ^{18}F-FDG PET/CT at baseline, with clinical and echocardiographic follow-up. The imaging protocols and image analysis techniques have been described previously (34). Twenty participants in this cohort had AV sclerosis (defined as an AV peak velocity between 1.5 and 2.5 m/s), but two participants were excluded from the current analysis due to missing echocardiographic data at baseline. One participant did not complete the ^{18}F-NaF uptake analysis, while another did not undergo ^{18}F-FDG uptake assessment.

Statistical analysis

Continuous variables are expressed as median (interquartile range) or mean ± standard deviation, while categorical variables are reported as frequencies and percentages. The normality of continuous variables was checked using the Shapiro-Wilk test. The characteristics of patient subgroups were compared using unpaired Student's t-test or Mann-Whitney U test

for continuous variables and Chi-squared or Fisher's exact test for categorical variables, as appropriate. The event-free survival of subgroups was visualized on Kaplan-Meier curves, and Log-rank tests were performed for comparison. Univariable and multivariable Cox proportional hazards models were used to compute hazard ratios (HRs) with 95% confidence intervals (CIs). To better understand the effects that the DL-predicted probability has on the primary endpoint, we computed pointwise estimates of the univariable and multivariable HR curves and the corresponding confidence limits using the smoothHR R package (35). The optimal degree of freedom was obtained by minimizing the corrected Akaike information criterion. The probability value where the lower bound of the confidence band of the multivariable HR intersects the HR of 1 was used as the cut-off value to discriminate between patients with high and low risk of developing AS. To demonstrate the incremental prognostic value of the DL-derived predictions over other conventional covariates, sequential (i.e., nested) Cox regression models were also constructed, which were then compared using the likelihood ratio test, Harrell's C-index (i.e., concordance index), integrated discrimination index (IDI), and net reclassification index (NRI). The final multivariable Cox regression model built using the ARIC dataset to predict the development of AS was applied to the external validation cohorts. We calculated the linear predictor as the weighted sum of the mean-centered independent variables (i.e., predictors) in the Cox regression model, where the weights were the regression coefficients (Supplemental Methods). Pearson's correlation coefficients were calculated to assess the strength of linear associations between the linear predictor and the ^{18}F-NaF and ^{18}F-FDG maximum and mean standardized uptake values (SUV).

A P-value of <0.05 was considered statistically significant. All statistical analyses were performed in R (version 4.1.2, R Foundation for Statistical Computing, Vienna, Austria). The utilized versions of the R packages are documented in Supplemental Table 3.

Ethical approval

All participants of the ARIC cohort study provided written informed consent, and the institutional review boards associated with each field center approved the study protocol. The two studies used for external validation (NCT01755936 and NCT01358513) were approved by the corresponding local research ethics committees, and written informed consent was obtained from all patients. The protocol of the current analysis conforms with the principles outlined in the Declaration of Helsinki, and it was approved by the Institutional Review Board of Rutgers Biomedical and Health Sciences (study identification number: Pro2021001505).

RESULTS

Clinical characteristics and outcomes of the participants in the ARIC cohort

Among the 5,576 participants (75 [71 – 79] years, 57% female, 19% black), 898 (16%) had AV sclerosis (Figure 1, Table 1). Over the median follow-up duration of 6.4 (5.7 – 6.9) years, 118 of 898 AV sclerosis patients (13%) developed AS, whereas 58 (6%) reached the composite endpoint. Of the 118 new diagnoses of AS, 72 (61%) were established using echocardiography, while the remaining were identified based on ICD codes.

Associations of the DL-derived predictions with outcomes in the ARIC cohort

The univariable and multivariable HR curves revealed that using the DL-predicted probability value of 0 as the reference, the risk of developing AS became significant at the probability value of 0.84 and 0.81, respectively, and continuously increased until the probability value of 1 (Figure 2). Using the latter as a cut-off, we assigned each subject either to the low-risk (probability of <0.81) or the high-risk group (probability of ≥ 0.81) (Table 1).

When we plotted and compared the event-free survival of the two groups, we observed that a higher proportion of high-risk compared to low-risk patients was diagnosed with AS and reached the composite endpoint during follow-up (Figure 3A). We could also observe a significant separation between the survival curves of the two risk groups when we used the default probability threshold of 0.5 (Figure 3B). Moreover, we also demonstrated in univariable Cox regression analysis that the DL-predicted probability is a significant predictor of both outcomes of interest (Tables 2 and 3). Using a multivariable Cox regression model including clinical variables and AV peak velocity as covariates, we also confirmed that the DL-predicted probability was an independent predictor of the new diagnosis of AS (Model AS3, Table 4). In addition, the probability values were also associated with this outcome of interest in

multivariable models that included several laboratory parameters or smoking status, chronic kidney disease, and medications besides AV peak velocity (Supplemental Tables 4 and 5). Although we could only include age, sex, race, and AV peak velocity as a covariate due to the limited number of participants reaching the composite endpoint, the DL-predicted probability was still found to be an independent predictor of this endpoint as well (Supplemental Table 6).

We also performed a sensitivity analysis by applying right censoring if the new diagnosis of AS was not ascertained by echocardiography and found that the DL-predicted probability of DD was still associated with the new diagnosis of AS (Supplemental Table 7).

The incremental value of DL-predicted DD probability over ASE/EACVI guideline-based DD grading is presented in the Supplementary Appendix (Supplemental Results, Supplemental Table 8, and Supplemental Figures 1 and 2).

Incremental prognostic value of the DL-derived predictions over conventional risk factors

In predicting the new diagnosis of AS, the DL-predicted probability of DD showed incremental prognostic value over clinical variables and AV peak velocity with significant improvement in Harrel's C-index, IDI, and NRI (Figure 4, Supplemental Table 9). It also had an incremental value over age, sex, race, and AV peak velocity for predicting the composite endpoint based on these three indices (Figure 4, Supplemental Table 10).

External validation

CMR cohort: A total of 50 patients with Stage B AS (24 with mild and 26 with moderate AS) underwent paired CMR and echocardiography at baseline and were followed up with annual echocardiographic examinations for two consecutive years. The baseline characteristics of this cohort are presented in Supplemental Tables 11 and 12. During the follow-up, 14 (28%) patients experienced a progression in AS severity (5 patients with mild AS developed moderate AS, 9 with moderate AS developed severe AS), and 5 required AV replacement. Patients classified into the high-risk group were more likely to experience progression in AS than patients in the low-risk group (Figure 5). Mid-wall LGE was observed in 7 (22%) patients in the high-risk group and 0 (0%) in the low-risk group (p=0.040), and patients with higher LGE-based myocardial fibrosis volumes and indexed extracellular volumes were more likely to be classified into the high-risk group (unadjusted OR: 1.161 [95% CI: 1.070 – 1.280], p=0.002, and 1.451 [95% CI: 1.199 – 1.867], p<0.001, respectively), even after adjusting for the severity of AS (adjusted OR: 1.147 [95% CI: 1.052 – 1.276], p=0.005, and 1.415 [95% CI: 1.161 – 1.825], p=0.002, respectively). When validated in the CMR cohort, the multivariable Cox model developed in the ARIC cohort (Model AS3, Table 4) predicted the progression of AS with a C-index of 0.798 [95% CI: 0.648 – 0.948], and the linear predictor calculated based on this model correlated positively with both the LGE-based myocardial fibrosis volume (r=0.48, p<0.001; Figure 6A) and the indexed extracellular volume (r=0.50, p<0.001; Figure 6B).

PET/CT cohort: The clinical characteristics of the PET/CT cohort are shown in Supplemental Table 13. All 18 patients were classified as high-risk. The linear predictor calculated using the final multivariable Cox regression model (Model AS3, Table 4) demonstrated a significant positive correlation with ^{18}F-NaF mean SUV (r=0.62, p=0.008; Figure 6C) and maximum SUV (r=0.56, p=0.020; Figure 6D); however, it did not correlate with ^{18}F-FDG mean SUV (r=0.15, p=0.558) or maximum SUV (r=0.07, p=0.797). The calculation

of the linear predictor is thoroughly described in the Supplemental Results, and examples are provided in Supplemental Table 14.

DISCUSSION

In 2014, the ACC/AHA valvular heart disease guideline introduced the patient-centered classification of AS, consisting of four stages. The first two stages, referring to early stages of subclinical AV disease, are highly prevalent, as indicated by recent data showing that Stages A (at risk of AS) and B (mild-to-moderate AS) are present in 39% and 17% of older adults, respectively (32). To the best of our knowledge, our current study is the first to investigate the associations between DL-predicted DD and the development and progression of AS in patients with early-stage (i.e., Stage A/B) AV disease (see Central Illustration).

The strength of our study is the utilization of data from various independent cohorts and validation using multimodality imaging. Initially, we applied our previously validated DL model on data from the ARIC cohort study, a population-based prospective study that included individuals from diverse regions of the US. In participants exhibiting AV sclerosis (Stage A), we determined the optimal DD probability threshold (0.81) for identifying individuals with high and low risk of progressing from AV sclerosis to AS. This threshold was subsequently used in an external cohort of patients with mild-to-moderate AS (Stage B) who underwent CMR imaging at baseline and annual echocardiographic assessments for two consecutive years. We found that high-risk patients had larger indexed extracellular volumes on CMR at baseline and were more likely to exhibit a progression in AS during follow-up than those classified into the low-risk group. These findings are consistent with those of previous studies in which a greater extent of diffuse myocardial fibrosis was associated with more severe DD and had additive value for predicting clinical outcomes in patients with AS (36).

Furthermore, in the ARIC cohort, we created a multivariable Cox model incorporating the DL-predicted probability of DD to predict the development of AS from AV sclerosis. The linear predictor calculated based on this multivariable Cox model demonstrated good discriminatory power in predicting the worsening of AS severity in the CMR cohort. Moreover,

in another external cohort, the linear predictor was also found to be positively correlated with baseline valvular ^{18}F-NaF mean and maximum SUV. Increased valvular calcification activity measured by ^{18}F-NaF uptake is known to be present in patients with AV sclerosis and has been shown to be an accurate predictor of disease progression, outperforming all baseline clinical and echocardiographic measures of AS severity (34,37,38). Overall, these findings suggest that the DL-based assessment of DD may identify an underlying milieu of valvular inflammation and calcification and myocardial fibrosis; thus, it can quantify the latent risk associated with the development and progression of AS.

The findings from our study bring to light several unresolved questions regarding myocardial changes in AS. For example, it has been previously believed that the excessive LV afterload in AS induces concentric hypertrophy and DD, and systolic function declines only later when the compensating mechanisms fail to maintain normal wall stress. Nevertheless, multiple studies have recently challenged this long-standing concept, showing that some patients may develop systolic dysfunction before AS becomes severe (39,40). Thus, LV systolic and diastolic dysfunction could occur even at the early stages of calcific AV disease (11). Our findings also support this observation and align with the mounting evidence that suggests mild AV disease (i.e., AV sclerosis and mild AS) occurs in a large proportion of patients with heart failure with preserved EF (HFpEF) (41).

Saliency maps and phenome-wide association studies supported links with traditional cardiovascular risk factors and diastolic dysfunction.

Our findings align with observations from a recent study proposing an innovative video-based biomarker for predicting the development and progression of AS (42). This biomarker was found to be correlated with multiple echocardiographic parameters of DD, and activation maps indicated that it also incorporated information from extra-valvular myocardial structures besides the AV (42). Building upon these observations and our study's findings, it is intriguing

to speculate that rather than being sequential phenomena, calcific AV disease and myocardial dysfunction may develop and progress concomitantly, and DD may even precede the development of AS. Previous studies have revealed that calcific AV disease is a highly regulated disease process mediated by several cellular and molecular pathways (43,44). Importantly, many of these pathways also play a central role in the pathophysiology of DD and HFpEF (45,46). For example, inflammation and oxidative stress are major factors contributing to the evolution of AS (47-49). These may be mediated by mitochondrial dysfunction and dysregulation of autophagy that extend even beyond the valve and underlie the development of adverse LV remodeling and DD (12-14). Thus, the identification of DD may capture this underlying systemic milieu of cellular impairment that affects both the valve and the myocardium.

Alternately, beyond being simply coexisting disease entities, it's also worthwhile speculating whether DD itself creates an environment that accelerates the progression of AV sclerosis. It is well-known that DD is associated with changes in the characteristics of intraventricular blood flow (50-53). Under physiological conditions, the intracavitary flow is redirected and accelerated toward the LV outflow during the pre-ejection period, forming a large anterior vortex and finally interacting with the AV leaflets as they open for LV ejection (50-52). Systolic and diastolic dysfunction disrupt this vortical blood flow (51,52,54), also altering the interaction of the blood flow with the AV. Interestingly, changes in blood flow dynamics have been linked to the accelerated progression of AV sclerosis to AS (55,56). Therefore, another plausible hypothesis could be that such DD-related changes alter shear stress on the AV – a key initiating factor in the development of calcific AV disease (44).

The clinical implications of identifying early-stage AS (Stage A/B) patients who have an increased risk of developing AS and subsequent progression are extraordinary. Although currently, there are no proven pharmacotherapies to prevent or halt the progression of AS,

discovering new pathways to mitigate the progression remains a hot topic for research. Multiple clinical trials are underway to investigate the pharmacological prevention of AS (57,58). AV sclerosis represents perhaps the ideal stage for intervention when the disease process is potentially most amenable to intervention; however, the fact that only 10-15% of patients develop AS has precluded trials in this population. The ability of our DL model to identify patients who are predisposed to progression could potentially facilitate candidate selection in clinical trials for pharmacologic interventions addressing the progression and development of AS.

Limitations

While our study has yielded promising results, it has several limitations that must be acknowledged. First, in our pursuit of complying with current recommendations (27), we opted to revise the upper limit of AV peak velocity from 2.0 to 2.5 m/s for defining AV sclerosis (59). Notably, this adjustment introduces a "gray zone" (AV peak velocity ranging from 2.0 to 2.5 m/s) where inconsistencies exist in guidelines concerning the terminology distinguishing AV sclerosis from mild AS. We recognize that further refinement of risk prediction could be achieved by defining the extent of calcification or valve thickening. Unfortunately, these were not reported during the echocardiographic examination at visit 5 in the ARIC cohort.

Second, it is noteworthy that the ARIC investigators also performed echocardiographic examinations during visit 7. However, the data from these examinations were not made publicly available at the time of our analysis. Therefore, we inferred the progression of AS based on ICD codes, a method with limitations yet frequently resorted to in epidemiological studies (60). Intriguingly, even a previously published study investigating the progression of Stage A/B AV disease based on serial echocardiographic assessment within the ARIC cohort necessitated the use of ICD codes because events such as AV replacements, hospitalizations, death, or being

lost to follow-up were frequent (32). To circumvent the unavailability of serial echocardiographic data for the ARIC cohort, we leveraged the validation offered by the independent CMR cohort, where patients underwent three echocardiographic examinations (one at baseline and two at annual follow-up visits), with only 5 patients being lost to follow-up. The consistency of our observations in both the ARIC and CMR cohorts substantiates the validity and generalizability of our DL model.

CONCLUSIONS

Based on our findings, we conclude that our DL model can efficiently integrate the echocardiographic features of DD and identify the latent risk associated with the development and progression of early-stage AS. Individualized modeling of AV disease trajectories and developing models for predicting disease progression has high clinical relevance for identifying patient subsets who will benefit from risk-mitigation strategies and therapeutic interventions that could potentially reduce the risk of AV disease development and progression.

CLINICAL PERSPECTIVES

COMPETENCY IN MEDICAL KNOWLEDGE:

Our DL model can efficiently integrate the echocardiographic features of DD to identify the latent risk associated with the development and progression of early-stage AS. The DL-predicted probability of DD correlated with the extent of myocardial fibrosis quantified using CMR imaging. Moreover, the predictions of the multivariable Cox regression model incorporating the DL-derived probability of DD correlated with valvular ^{18}F-NaF uptake assessed by PET/CT, thereby identifying a milieu of valvular inflammation and calcification that is known to be associated with the progression of calcific AV disease.

TRANSLATIONAL OUTLOOK:

Given its ability to identify patients with early-stage AS who are prone to progression, our DL model has the potential to aid in targeting novel pharmacotherapies to those who are most likely to see a benefit. Thus, by optimizing candidate selection and enabling the timely initiation of pharmacologic treatment, DL-based tools could accelerate the development of long-awaited medical therapies for calcific AV disease.

REFERENCES

1. Coffey S, Cox B, Williams MJ. The prevalence, incidence, progression, and risks of aortic valve sclerosis: a systematic review and meta-analysis. J Am Coll Cardiol 2014;63:2852-61.
2. Freeman RV, Otto CM. Spectrum of Calcific Aortic Valve Disease. Circulation 2005;111:3316-3326.
3. Faggiano P, Antonini-Canterin F, Erlicher A et al. Progression of aortic valve sclerosis to aortic stenosis. American Journal of Cardiology 2003;91:99-101.
4. Cosmi JE, Kort S, Tunick PA et al. The risk of the development of aortic stenosis in patients with "benign" aortic valve thickening. Arch Intern Med 2002;162:2345-7.
5. Barasch E, Gottdiener JS, Tressel W et al. The Associations of Aortic Valve Sclerosis, Aortic Annular Increased Reflectivity, and Mitral Annular Calcification with Subsequent Aortic Stenosis in Older Individuals: Findings from the Cardiovascular Health Study. J Am Soc Echocardiogr 2023;36:41-49.e1.
6. Nightingale AK, Horowitz JD. Aortic sclerosis: not an innocent murmur but a marker of increased cardiovascular risk. Heart 2005;91:1389-93.
7. Otto CM, Nishimura RA, Bonow RO et al. 2020 ACC/AHA Guideline for the Management of Patients With Valvular Heart Disease: A Report of the American College of Cardiology/American Heart Association Joint Committee on Clinical Practice Guidelines. Circulation 2021;143:e72-e227.
8. Stewart BF, Siscovick D, Lind BK et al. Clinical Factors Associated With Calcific Aortic Valve Disease. Journal of the American College of Cardiology 1997;29:630-634.

9. Eveborn GW, Schirmer H, Lunde P, Heggelund G, Hansen J-B, Rasmussen K. Assessment of risk factors for developing incident aortic stenosis: the Tromsø Study. European Journal of Epidemiology 2014;29:567-575.

10. Kosmala W, Marwick TH. Asymptomatic Left Ventricular Diastolic Dysfunction: Predicting Progression to Symptomatic Heart Failure. JACC: Cardiovascular Imaging 2020;13:215-227.

11. Yoshida Y, Nakanishi K, Daimon M et al. Aortic valve sclerosis and subclinical left ventricular dysfunction in the general population with normal left ventricular geometry. European Journal of Preventive Cardiology 2022.

12. Zhang S, Liu C, Zhang Y et al. Different heart failure phenotypes of valvular heart disease: the role of mitochondrial dysfunction. Front Cardiovasc Med 2023;10:1135938.

13. Pedriali G, Morciano G, Patergnani S et al. Aortic Valve Stenosis and Mitochondrial Dysfunctions: Clinical and Molecular Perspectives. Int J Mol Sci 2020;21.

14. Lozhkin A, Vendrov AE, Ramos-Mondragón R et al. Mitochondrial oxidative stress contributes to diastolic dysfunction through impaired mitochondrial dynamics. Redox Biol 2022;57:102474.

15. Dai W, Nazzari H, Namasivayam M, Hung J, Stultz CM. Identifying Aortic Stenosis With a Single Parasternal Long-Axis Video Using Deep Learning. J Am Soc Echocardiogr 2023;36:116-118.

16. Yang F, Chen X, Lin X et al. Automated Analysis of Doppler Echocardiographic Videos as a Screening Tool for Valvular Heart Diseases. JACC: Cardiovascular Imaging 2022;15:551-563.

17. Wessler BS, Huang Z, Long GM, Jr. et al. Automated Detection of Aortic Stenosis Using Machine Learning. J Am Soc Echocardiogr 2023;36:411-420.

18. Namasivayam M, Myers PD, Guttag JV et al. Predicting outcomes in patients with aortic stenosis using machine learning: the Aortic Stenosis Risk (ASteRisk) score. Open Heart 2022;9.

19. Sánchez-Puente A, Dorado-Díaz PI, Sampedro-Gómez J et al. Machine-learning to Optimize the Echocardiographic Follow-up of Aortic Stenosis. JACC Cardiovasc Imaging 2023.

20. Cohen-Shelly M, Attia ZI, Friedman PA et al. Electrocardiogram screening for aortic valve stenosis using artificial intelligence. Eur Heart J 2021;42:2885-2896.

21. Ito S, Cohen-Shelly M, Attia ZI et al. Correlation between artificial intelligence-enabled electrocardiogram and echocardiographic features in aortic stenosis. Eur Heart J Digit Health 2023;4:196-206.

22. Kwon JM, Lee SY, Jeon KH et al. Deep Learning-Based Algorithm for Detecting Aortic Stenosis Using Electrocardiography. J Am Heart Assoc 2020;9:e014717.

23. Hata E, Seo C, Nakayama M, Iwasaki K, Ohkawauchi T, Ohya J. Classification of Aortic Stenosis Using ECG by Deep Learning and its Analysis Using Grad-CAM. Annu Int Conf IEEE Eng Med Biol Soc 2020;2020:1548-1551.

24. Holste G, Oikonomou EK, Mortazavi BJ et al. Severe aortic stenosis detection by deep learning applied to echocardiography. European Heart Journal 2023;44:4592-4604.

25. Wright JD, Folsom AR, Coresh J et al. The ARIC (Atherosclerosis Risk In Communities) Study: JACC Focus Seminar 3/8. Journal of the American College of Cardiology 2021;77:2939-2959.

26. Shah AM, Cheng S, Skali H et al. Rationale and design of a multicenter echocardiographic study to assess the relationship between cardiac structure and function and heart failure risk in a biracial cohort of community-dwelling elderly

persons: the Atherosclerosis Risk in Communities study. Circ Cardiovasc Imaging 2014;7:173-81.

27. Baumgartner H, Hung J, Bermejo J et al. Recommendations on the Echocardiographic Assessment of Aortic Valve Stenosis: A Focused Update from the European Association of Cardiovascular Imaging and the American Society of Echocardiography. J Am Soc Echocardiogr 2017;30:372-392.

28. Nagueh SF, Smiseth OA, Appleton CP et al. Recommendations for the Evaluation of Left Ventricular Diastolic Function by Echocardiography: An Update from the American Society of Echocardiography and the European Association of Cardiovascular Imaging. J Am Soc Echocardiogr 2016;29:277-314.

29. Tokodi M, Shrestha S, Bianco C et al. Interpatient Similarities in Cardiac Function: A Platform for Personalized Cardiovascular Medicine. JACC Cardiovasc Imaging 2020;13:1119-1132.

30. Pandey A, Kagiyama N, Yanamala N et al. Deep-Learning Models for the Echocardiographic Assessment of Diastolic Dysfunction. JACC Cardiovasc Imaging 2021;14:1887-1900.

31. https://wvu-model.herokuapp.com.

32. Shelbaya K, Claggett B, Dorbala P et al. Stages of Valvular Heart Disease Among Older Adults in the Community: The Atherosclerosis Risk in Communities Study. Circulation 2023;147:638-649.

33. Chin CWL, Everett RJ, Kwiecinski J et al. Myocardial Fibrosis and Cardiac Decompensation in Aortic Stenosis. JACC Cardiovasc Imaging 2017;10:1320-1333.

34. Dweck MR, Jones C, Joshi NV et al. Assessment of valvular calcification and inflammation by positron emission tomography in patients with aortic stenosis. Circulation 2012;125:76-86.

35. Meira-Machado L, Cadarso-Suárez C, Gude F, Araújo A. smoothHR: An R Package for Pointwise Nonparametric Estimation of Hazard Ratio Curves of Continuous Predictors. Computational and Mathematical Methods in Medicine 2013;2013:745742.

36. Lee HJ, Lee H, Kim SM et al. Diffuse Myocardial Fibrosis and Diastolic Function in Aortic Stenosis. JACC Cardiovasc Imaging 2020;13:2561-2572.

37. Dweck MR, Jenkins WS, Vesey AT et al. 18F-sodium fluoride uptake is a marker of active calcification and disease progression in patients with aortic stenosis. Circ Cardiovasc Imaging 2014;7:371-8.

38. Jenkins WS, Vesey AT, Shah AS et al. Valvular (18)F-Fluoride and (18)F-Fluorodeoxyglucose Uptake Predict Disease Progression and Clinical Outcome in Patients With Aortic Stenosis. J Am Coll Cardiol 2015;66:1200-1.

39. Casaclang-Verzosa G, Shrestha S, Khalil MJ et al. Network Tomography for Understanding Phenotypic Presentations in Aortic Stenosis. JACC Cardiovasc Imaging 2019;12:236-248.

40. Ito S, Miranda WR, Nkomo VT et al. Reduced Left Ventricular Ejection Fraction in Patients With Aortic Stenosis. J Am Coll Cardiol 2018;71:1313-1321.

41. Verbrugge FH, Reddy YNV, Eleid MF, Lin G, Burkhoff D, Borlaug BA. Mild aortic valve disease and the diastolic pressure-volume relationship in heart failure with preserved ejection fraction. Open Heart 2021;8.

42. Oikonomou EK, Holste G, Yuan N et al. A Multimodal Video-Based AI Biomarker for Aortic Stenosis Development and Progression. JAMA Cardiol 2024.

43. Lerman DA, Prasad S, Alotti N. Calcific Aortic Valve Disease: Molecular Mechanisms and Therapeutic Approaches. Eur Cardiol 2015;10:108-112.

44. Otto CM. Calcific Aortic Stenosis — Time to Look More Closely at the Valve. New England Journal of Medicine 2008;359:1395-1398.

45. Borlaug BA, Sharma K, Shah SJ, Ho JE. Heart Failure With Preserved Ejection Fraction. Journal of the American College of Cardiology 2023;81:1810-1834.

46. Mishra S, Kass DA. Cellular and molecular pathobiology of heart failure with preserved ejection fraction. Nature Reviews Cardiology 2021;18:400-423.

47. Greenberg HZE, Zhao G, Shah AM, Zhang M. Role of oxidative stress in calcific aortic valve disease and its therapeutic implications. Cardiovascular Research 2021;118:1433-1451.

48. Dweck MR, Boon NA, Newby DE. Calcific Aortic Stenosis: A Disease of the Valve and the Myocardium. Journal of the American College of Cardiology 2012;60:1854-1863.

49. Driscoll K, Cruz AD, Butcher JT. Inflammatory and Biomechanical Drivers of Endothelial-Interstitial Interactions in Calcific Aortic Valve Disease. Circ Res 2021;128:1344-1370.

50. Sengupta PP, Khandheria BK, Korinek J et al. Left ventricular isovolumic flow sequence during sinus and paced rhythms: new insights from use of high-resolution Doppler and ultrasonic digital particle imaging velocimetry. J Am Coll Cardiol 2007;49:899-908.

51. Zhang H, Zhang J, Zhu X et al. The left ventricular intracavitary vortex during the isovolumic contraction period as detected by vector flow mapping. Echocardiography 2012;29:579-87.

52. Li Q, Huang L, Ma N et al. Relationship between left ventricular vortex and preejectional flow velocity during isovolumic contraction studied by using vector flow mapping. Echocardiography 2019;36:558-566.

53. Schäfer M, Humphries S, Stenmark KR et al. 4D-flow cardiac magnetic resonance-derived vorticity is sensitive marker of left ventricular diastolic dysfunction in patients

with mild-to-moderate chronic obstructive pulmonary disease. European Heart Journal - Cardiovascular Imaging 2017;19:415-424.

54. Hong GR, Pedrizzetti G, Tonti G et al. Characterization and quantification of vortex flow in the human left ventricle by contrast echocardiography using vector particle image velocimetry. JACC Cardiovasc Imaging 2008;1:705-17.

55. Vogl BJ, Niemi NR, Griffiths LG, Alkhouli MA, Hatoum H. Impact of calcific aortic valve disease on valve mechanics. Biomechanics and Modeling in Mechanobiology 2022;21:55-77.

56. Sun L, Rajamannan NM, Sucosky P. Defining the Role of Fluid Shear Stress in the Expression of Early Signaling Markers for Calcific Aortic Valve Disease. PLOS ONE 2013;8:e84433.

57. Chong T, Lan NSR, Courtney W et al. Medical Therapy to Prevent or Slow Progression of Aortic Stenosis: Current Evidence and Future Directions. Cardiol Rev 2023.

58. Lindman BR, Sukul D, Dweck MR et al. Evaluating Medical Therapy for Calcific Aortic Stenosis: JACC State-of-the-Art Review. Journal of the American College of Cardiology 2021;78:2354-2376.

59. Sengeløv M, Cheng S, Biering-Sørensen T et al. Ideal Cardiovascular Health and the Prevalence and Severity of Aortic Stenosis in Elderly Patients. J Am Heart Assoc 2018;7.

60. Strom JB, Xu J, Sun T et al. Characterizing the Accuracy of International Classification of Diseases, Tenth Revision Administrative Claims for Aortic Valve Disease. Circ Cardiovasc Qual Outcomes 2022;15:e009162.

Table 1 Clinical and echocardiographic characteristics of patients with high and low risk of progressing to AS in the ARIC cohort

	Missing n (%)	All participants with AV sclerosis n=898	High-risk group n=346	Low-risk group n=552	P-value
Demographics, vitals, risk factors					
Age, years	0 (0)	76 (72 – 80)	77 (73 – 82)	75 (71 – 79)	<0.001
Male sex	0 (0)	404 (45)	174 (50)	230 (42)	0.014
Black race	0 (0)	152 (17)	71 (21)	81 (15)	0.029
BMI, kg/m^2	3 (0)	28.9 (25.9 – 33.1)	29.9 (26.3 – 34.4)	28.5 (25.7 – 32.7)	0.003
BSA, m^2	0 (0)	1.89 (1.74 – 2.04)	1.93 (1.77 – 2.08)	1.88 (1.73 – 2.03)	0.020
SBP, mmHg	2 (0)	130 (119 – 142)	133 (119 – 146)	128 (119 – 140)	0.009
DBP, mmHg	2 (0)	65 (58 – 72)	65 (57 – 73)	65 (58 – 71)	0.812
HR, 1/min	2 (0)	63 (57 – 71)	62 (55 – 70)	64 (58 – 71)	0.007
Hypertension	0 (0)	769 (86)	315 (91)	454 (82)	<0.001
Diabetes	0 (0)	353 (39)	156 (45)	197 (36)	0.006
Chronic kidney disease	0 (0)	283 (32)	135 (39)	148 (27)	<0.001
Smoking status	66 (7)				
Never smoker		335 (40)	122 (39)	213 (41)	
Current smoker		47 (6)	17 (5)	30 (6)	
Former smoker		450 (54)	177 (56)	273 (53)	0.695
History of HF	0 (0)	163 (18)	103 (30)	60 (11)	<0.001
History of CHD	0 (0)	179 (20)	101 (29)	78 (14)	<0.001
History of AF	0 (0)	95 (11)	61 (18)	34 (6)	<0.001
History of stroke	0 (0)	60 (7)	33 (10)	27 (5)	0.010
Medications					
Antihypertensive medications	0 (0)	718 (80)	299 (86)	419 (76)	<0.001
Antidiabetic medications	3 (0)	195 (22)	97 (28)	98 (18)	<0.001
Statin	6 (1)	512 (57)	203 (59)	309 (56)	0.434
Cholesterol-lowering medications	6 (1)	558 (63)	221 (64)	337 (61)	0.399
Laboratory results					
Creatinine, mg/dL	5 (1)	0.93 (0.79 – 1.12)	0.98 (0.82 – 1.19)	0.91 (0.77 – 1.07)	<0.001
GFR, mL/min/1.73m^2	5 (1)	70 (58 – 82)	68 (54 – 81)	70 (60 – 84)	0.001
Uric acid, mg/dL	5 (1)	5.8 (4.9 – 6.7)	5.9 (4.9 – 7.0)	5.7 (4.8 – 6.6)	0.095
Fasting glucose, mg/dL	11 (1)	107 (98 – 122)	109 (98 – 125)	106 (98 – 120)	0.128
Hemoglobin A1C, %	7 (1)	5.7 (5.5 – 6.1)	5.8 (5.5 – 6.4)	5.7 (5.5 – 6.0)	0.006
Triglyceride, mg/dL	6 (1)	112 (85 – 156)	109 (83 – 148)	113 (87 – 158)	0.128
Total chol., mg/dL	6 (1)	174 (150 – 201)	166 (136 – 197)	179 (155 – 204)	<0.001
LDL-C, mg/dL	12 (1)	98 (77 – 122)	93 (69 – 121)	102 (81 – 123)	<0.001
HDL-C, mg/dL	6 (1)	50 (41 – 58)	48 (39 – 56)	51 (42 – 58)	<0.001
NT-proBNP, pg/mL	29 (3)	143 (75 – 290)	240 (114 – 478)	113 (65 – 205)	<0.001
hs-Troponin T, ng/mL	5 (1)	0.01 (0.01 – 0.02)	0.01 (0.01 – 0.02)	0.01 (0.01 – 0.01)	<0.001
hs-CRP, mg/dL	6 (1)	2.17 (1.03 – 4.60)	2.33 (1.20 – 4.87)	2.07 (1.01 – 4.35)	0.123
Hemoglobin, g/dL	27 (3)	13.3 (12.4 – 14.3)	13.3 (12.4 – 14.3)	13.4 (12.5 – 14.3)	0.524
RDW, %	27 (3)	14.2 (13.6 – 15.0)	14.3 (13.6 – 15.0)	14.2 (13.6 – 14.9)	0.124
Echocardiographic parameters					
IVSd, cm	0 (0)	1.05 (0.95 – 1.18)	1.15 (1.02 – 1.26)	1.00 (0.93 – 1.12)	<0.001
LVPWd, cm	0 (0)	0.94 (0.87 – 1.03)	1.01 (0.92 – 1.13)	0.90 (0.85 – 0.97)	<0.001
LVIDd, cm	0 (0)	4.48 ± 0.53	4.70 ± 0.56	4.35 ± 0.47	<0.001
LVIDs, cm	0 (0)	2.60 (2.25 – 2.95)	2.79 (2.38 – 3.19)	2.51 (2.17 – 2.80)	<0.001
LVMi, g/m^2	0 (0)	79.9 (69.2 – 94.9)	95.5 (81.5 – 110.)	73.3 (65.6 – 83.0)	<0.001
LVEDVi, mL/m^2	0 (0)	44.1 (37.5 – 51.3)	48.43 (41.3 – 56.1)	41.58 (36.1 – 48.6)	<0.001
LVESVi, mL/m^2	0 (0)	14.4 (11.5 – 18.1)	17.2 (13.9 – 21.3)	13.2 (10.8 – 15.9)	<0.001
LVEF, %	0 (0)	67.1 (62.7 – 70.8)	63.9 (60.0 – 68.3)	68.3 (65.4 – 71.7)	<0.001
LVGLS, %	30 (3)	-18.6 (-20.1 to -16.8)	-17.5 (-19.2 to -15.7)	-19.1 (-20.4 to -17.7)	<0.001
LAVi, mL/m^2	0 (0)	26.9 (22.4 – 32.5)	31.1 (25.7 – 37.6)	24.9 (21.0 – 29.7)	<0.001

Table 1 Continued

	Missing n (%)	**All participants with AV sclerosis** n=898	**Participants with events** n=346	**Participants without events** n=552	**P-value**
AV peak velocity, m/s	0 (0)	1.66 (1.56 – 1.86)	1.67 (1.55 – 1.89)	1.65 (1.56 – 1.84)	0.245
AV mean gradient, mmHg	0 (0)	5.2 (4.5 – 6.5)	5.4 (4.6 – 6.7)	5.2 (4.5 – 6.3)	0.023
Dimensionless index	0 (0)	0.68 (0.57 – 0.78)	0.64 (0.52 – 0.74)	0.70 (0.59 – 0.81)	<0.001
E, cm/s	0 (0)	71 (60 – 83)	75 (61 – 89)	70 (59 – 80)	<0.001
E/A	35 (4)	0.8 (0.7 – 1.0)	0.8 (0.6 – 0.9)	0.8 (0.7 – 1.0)	0.028
e' (septal), cm/s	0 (0)	5.6 (4.8 – 6.6)	4.8 (4.1 – 5.3)	6.2 (5.3 – 7.2)	<0.001
E/e' (septal)	0 (0)	12.4 (10.2 – 15.6)	15.5 (12.7 – 19.4)	11.04 (9.5 – 13.1)	<0.001
TRV, m/s	334 (37)	2.45 (2.25 – 2.65)	2.49 (2.25 – 2.73)	2.42 (2.25 – 2.60)	0.004
Guideline-based DD	0 (0)				
No DD		222 (25)	30 (9)	192 (35)	
Grade I		459 (51)	179 (52)	280 (51)	
Grade II		78 (9)	64 (18)	14 (3)	
Grade III		6 (1)	6 (2)	0 (0)	
Indeterminate		133 (15)	67 (19)	66 (12)	<0.001
DL-predicted probability of DD	0 (0)	0.50 (0.04 – 0.97)	0.99 (0.94 – 1.00)	0.07 (0.01 – 0.38)	<0.001
DL-predicted high risk	0 (0)	346 (39)	346 (100)	0 (0)	<0.001

Continuous variables are presented as median (interquartile range) and categorical variables as n (%). Comparisons between the high-risk and low-risk phenogroups were performed using unpaired Student's t-test or Mann-Whitney U test for continuous variables, Chi-squared or Fisher's exact test for categorical variables, as appropriate.

A – late mitral inflow velocity, AF – atrial fibrillation, ARIC – Atherosclerosis Risk in Communities study, AS – aortic stenosis, AV – aortic valve, BMI – body mass index, BSA – body surface area, CHD – coronary heart disease, CRP – C-reactive protein, DBP – diastolic blood pressure, DD – diastolic dysfunction, DL – deep learning, E – early mitral inflow velocity, e' – early diastolic mitral annular velocity, GFR – glomerular filtration rate, HDL-C – high-density lipoprotein cholesterol, HF – heart failure, HR – heart rate, hs – high-sensitivity, IVSd – thickness of the interventricular septum at end-diastole, LAVi – left atrial volume index, LDL-C – low-density lipoprotein cholesterol, LVEDVi – left ventricular end-diastolic volume index, LVEF – left ventricular ejection fraction, LVESVi – left ventricular end-systolic volume index, LVIDd – left ventricular internal diameter at end-diastole, LVIDs – left ventricular internal diameter at end-systole, LVGLS – left ventricular global longitudinal strain, LVMi – left ventricular mass index, LVPWd – thickness of the left ventricular posterior wall at end-diastole, NT-proBNP – N-terminal pro-brain natriuretic peptide, RDW – red cell distribution width, SBP – systolic blood pressure, TRV –tricuspid regurgitation peak velocity

Table 2 Univariable Cox regression models for predicting the new diagnosis of AS in patients with AV sclerosis in the ARIC cohort

	N	HR [95% CI]	P-value
Demographics and risk factors			
Age	898	1.082 [1.046 – 1.120]	<0.001
Male sex	898	1.551 [1.079 – 2.229]	0.018
Black race	898	0.397 [0.193 – 0.815]	0.012
Hypertension	898	2.197 [1.113 – 4.336]	0.023
Diabetes	898	1.818 [1.267 – 2.610]	0.001
Chronic kidney disease	898	1.923 [1-338 – 2.764]	<0.001
Smoking status	832		
Current smoker		1.286 [0.577 – 2.867]	0.538
Former smoker		1.178 [0.794 – 1.748]	0.416
History of HF	898	2.741 [1.861 – 4.039]	<0.001
History of CHD	898	2.495 [1.707 – 3.645]	<0.001
History of AF	898	2.341 [1.472 – 3.722]	<0.001
History of stroke	898	1.748 [0.962 – 3.175]	0.067
Medications			
Antihypertensive medication	898	2.005 [1.148 – 3.503]	0.015
Antidiabetic medication	895	1.688 [1.141 – 2.499]	0.009
Statin	892	1.351 [0.927 – 1.970]	0.117
Cholesterol-lowering medication	892	1.414 [0.953 – 2.099]	0.086
Laboratory results			
Creatinine	893	1.434 [1.181 – 1.741]	<0.001
GFR	893	0.983 [0.973 – 0.992]	<0.001
Uric acid	893	1.109 [0.977 – 1.259]	0.108
Fasting glucose	887	1.005 [1.000 – 1.011]	0.046
Hemoglobin A1C	891	1.278 [1.068 – 1.530]	0.008
Triglyceride	892	1.002 [1.000 – 1.005]	0.075
Total cholesterol	892	0.997 [0.992 – 1.001]	0.171
LDL-C	886	0.997 [0.991 – 1.002]	0.264
HDL-C	892	0.975 [0.959 – 0.990]	0.002
Log_{10}(NT-proBNP)	869	5.993 [4.155 – 8.644]	<0.001
Log_{10}(hs-Troponin T)	893	6.048 [3.310 – 11.053]	<0.001
hs-CRP	892	0.998 [0.974 – 1.023]	0.886
Hemoglobin	871	1.035 [0.911 – 1.176]	0.599
RDW	871	1.178 [1.004 – 1.382]	0.045
Echocardiographic parameters			
LVMi	898	1.019 [1.013 – 1.025]	<0.001
LVEDVi	898	1.029 [1.015 – 1.044]	<0.001
LVESVi	898	1.051 [1.036 – 1.067]	<0.001
LVEF	898	0.933 [0.915 – 0.953]	<0.001
LVGLS	868	1.192 [1.121 – 1.268]	<0.001
LAVi	898	1.020 [1.012 – 1.027]	<0.001
AV peak velocity	898	9.915 [5.403 – 18.195]	<0.001
AV mean gradient	898	1.344 [1.255 – 1.439]	<0.001
Dimensionless index	898	0.003 [0.001 – 0.011]	<0.001
E	898	1.011 [1.002 – 1.020]	0.014
E/A	863	0.873 [0.400 – 1.909]	0.734
e' (septal)	898	0.775 [0.674 – 0.891]	<0.001
E/e' (septal)	898	1.087 [1.054 – 1.121]	<0.001
TRV	564	1.701 [0.841 – 3.441]	0.139
Guideline-based DD	898		
Grade I		1.862 [1.086 – 3.191]	0.024
Grade II		3.914 [2.034 – 7.532]	<0.001
Grade III		15.477 [5.197 – 46.091]	<0.001
Indeterminate		1.947 [1.003 – 3.779]	0.049
DL-predicted probability of DD	898	5.399 [3.253 – 8.962]	<0.001

CI – confidence interval, HR – hazard ratio; other abbreviations as in Table 1.

Table 3 Univariable and multivariable Cox regression models for predicting the composite endpoint in patients with AV sclerosis in the ARIC cohort

	N	HR [95% CI]	P-value
Demographics and risk factors			
Age	898	1.123 [1.069 – 1.179]	<0.001
Male sex	898	1.525 [0.909 – 2.559]	0.110
Black race	898	0.215 [0.052 – 0.884]	0.033
Hypertension	898	2.420 [0.876 – 6.682]	0.088
Diabetes	898	2.163 [1.289 – 3.630]	0.004
Chronic kidney disease	898	2.700 [1.612 – 4.524]	<0.001
Smoking status	832		
Current smoker		0.689 [0.162 – 2.937]	0.614
Former smoker		1.080 [0.616 – 1.893]	0.789
History of HF	898	4.734 [2.817 – 7.957]	<0.001
History of CHD	898	2.711 [1.595 – 4.608]	<0.001
History of AF	898	2.651 [1.404 – 5.006]	0.003
History of stroke	898	2.484 [1.178 – 5.240]	0.017
Medications			
Antihypertensive medication	898	1.658 [0.786 – 3.497]	0.184
Antidiabetic medication	895	1.713 [0.982 – 2.989]	0.058
Statin	892	1.383 [0.805 – 2.377]	0.240
Cholesterol-lowering medication	892	1.521 [0.855 – 2.705]	0.154
Laboratory results			
Creatinine	893	1.566 [1.244 – 1.972]	<0.001
GFR	893	0.976 [0.962 – 0.989]	<0.001
Uric acid	893	1.090 [0.909 – 1.307]	0.351
Fasting glucose	887	1.004 [0.997 – 1.012]	0.274
Hemoglobin A1C	891	1.290 [1.003 – 1.658]	0.047
Triglyceride	892	1.001 [0.998 – 1.005]	0.386
Total cholesterol	892	0.991 [0.984 – 0.998]	0.011
LDL-C	886	0.988 [0.979 – 0.997]	0.006
HDL-C	892	0.967 [0.944 – 0.990]	0.006
Log_{10}(NT-proBNP)	869	9.864 [5.988 – 16.251]	<0.001
Log_{10}(hs-Troponin T)	893	17.631 [7.766 – 40.026]	<0.001
hs-CRP	892	1.011 [0.985 – 1.038]	0.399
Hemoglobin	871	1.009 [0.843 – 1.208]	0.919
RDW	871	1.354 [1.101 – 1.665]	0.004
Echocardiographic parameters			
LVMi	898	1.023 [1.016 – 1.030]	<0.001
LVEDVi	898	1.032 [1.012 – 1.052]	0.001
LVESVi	898	1.056 [1.034 – 1.079]	<0.001
LVEF	898	0.933 [0.909 – 0.959]	<0.001
LVGLS	868	1.224 [1.125 – 1.332]	<0.001
LAVi	898	1.022 [1.012 – 1.033]	<0.001
AV peak velocity	898	14.136 [6.036 – 33.104]	<0.001
AV mean gradient	898	1.396 [1.270 – 1.534]	<0.001
Dimensionless index	898	0.002 [0.000 – 0.010]	<0.001
E	898	1.019 [1.008 – 1.030]	<0.001
E/A	863	0.861 [0.292 – 2.544]	0.787
e' (septal)	898	0.697 [0.568 – 0.855]	<0.001
E/e' (septal)	898	1.123 [1.078 – 1.170]	<0.001
TRV	564	2.079 [0.759 – 5.699]	0.155
Guideline-based DD	898		
Grade I		2.251 [0.988 – 5.125]	0.053
Grade II		3.883 [1.408 – 10.710]	0.009
Grade III		11.388 [2.364 – 54.864]	0.002
Indeterminate vs. no DD		2.944 [1.141 – 7.594]	0.026
DL-predicted probability of DD	898	9.886 [4.300 – 22.727]	<0.001

Abbreviations as in Tables 1 and 2.

Table 4 Sequential multivariable Cox regression models for predicting the new diagnosis of AS in patients with AV sclerosis in the ARIC cohort

	Model AS1 (C-index: 0.709, AIC: 1,498)		**Model AS2** (C-index: 0.747, AIC: 1,469)		**Model AS3** (C-index: 0.773, AIC: 1,446)	
	HR [95% CI]	**P-value**	**HR [95% CI]**	**P-value**	**HR [95% CI]**	**P-value**
Age, years	1.061 [1.025 – 1.099]	<0.001	1.054 [1.019 – 1.091]	0.002	1.043 [1.008 – 1.079]	0.017
Male sex	1.179 [0.806 – 1.726]	0.397	1.074 [0.728 – 1.584]	0.720	1.007 [0.680 – 1.490]	0.974
Black race	0.353 [0.169 – 0.738]	0.006	0.383 [0.183 – 0.804]	0.011	0.367 [0.174 – 0.772]	0.008
Hypertension	1.781 [0.892 – 3.555]	0.102	1.632 [0.817 – 3.260]	0.165	1.471 [0.735 – 2.945]	0.276
Diabetes	1.569 [1.085 – 2.268]	0.017	1.555 [1.075 – 2.250]	0.019	1.474 [1.016 – 2.139]	0.041
History of HF	2.125 [1.373 – 3.289]	<0.001	2.045 [1.331 – 3.143]	0.001	1.784 [1.160 – 2.742]	0.008
History of CHD	1.427 [0.928 – 2.195]	0.106	1.309 [0.850 – 2.016]	0.221	1.210 [0.783 – 1.868]	0.391
History of AF	1.474 [0.912 – 2.384]	0.114	1.419 [0.881 – 2.283]	0.150	1.328 [0.828 – 2.130]	0.240
AV peak velocity, m/s			6.412 [3.427 – 11.998]	<0.001	5.689 [3.075 – 10.524]	<0.001
DL-predicted probability of DD					3.482 [2.061 – 5.884]	<0.001

AIC – Akaike information criterion; other abbreviations as in Tables 1 and 2.

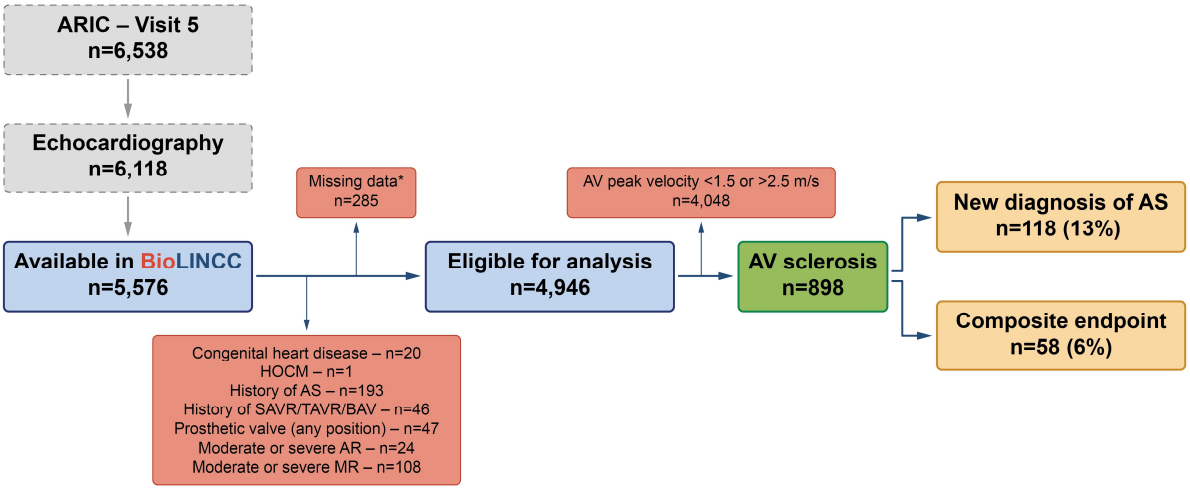

Figure 1 Patient selection flowchart of the ARIC cohort

*Missing values in key echocardiographic variables or no follow-up data.

Of the 4,946 participants eligible for analysis, 3,987 (81%) had an AV peak velocity lower than 1.5 m/s, and 61 (1%) had an AV peak velocity higher than 2.5 m/s at visit 5.

AR – aortic regurgitation, ARIC – Atherosclerosis Risk in Communities study, AS – aortic stenosis, AV – aortic valve, BAV – bicuspid aortic valve, BioLINCC – Biologic Specimen and Data Repository Information Coordinating Center, HOCM – hypertrophic obstructive cardiomyopathy, MR – mitral regurgitation, SAVR – surgical aortic valve replacement, TAVR – transcatheter aortic valve replacement

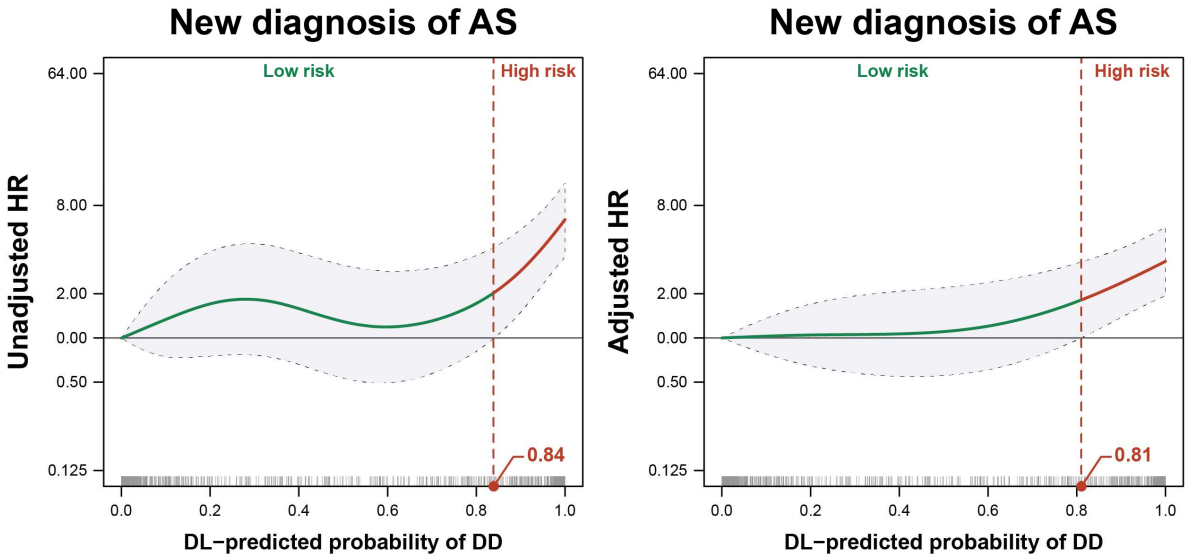

Figure 2 The dependence of the risk of developing AS on the DL-predicted probability of DD in the ARIC cohort

The probability value of 0 was taken as the reference. The red vertical dashed line indicates the probability value where the lower bound of the confidence band intersects the HR of 1.

DD – diastolic dysfunction, DL – deep learning, HR – hazard ratio; other abbreviations as in Figure 1.

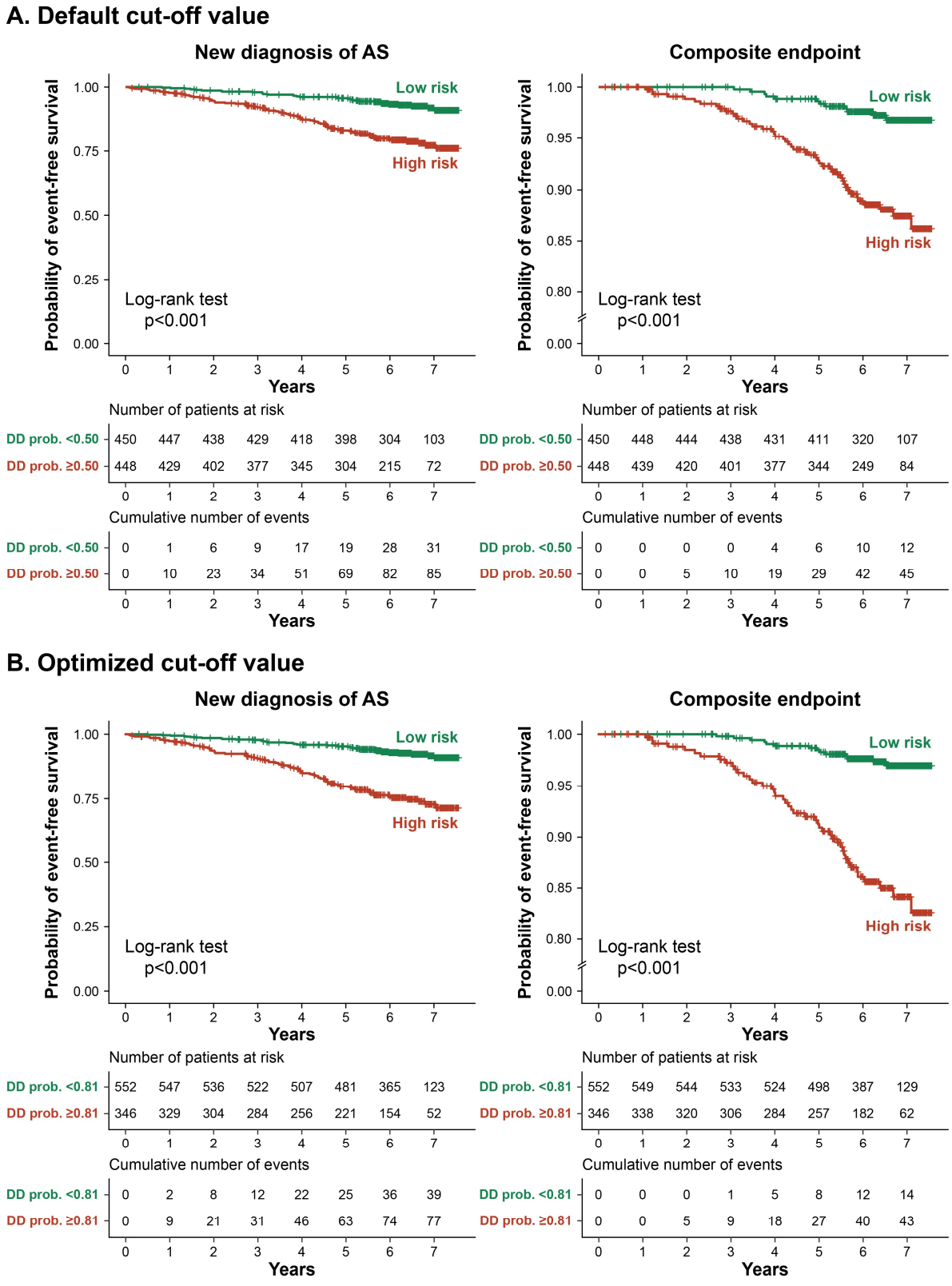

Figure 3 Kaplan-Meier curves showing the event-free survival of patients with AV sclerosis in the ARIC cohort

In panel A, the default cut-off value (i.e., the DD probability value of 0.50) was used to stratify patients into low-risk and high-risk groups. In panel B, the cut-off value optimized in the ARIC cohort (i.e., the DD probability value of 0.81) was used to stratify patients into low-risk and high-risk groups.

Abbreviations as in Figure 1.

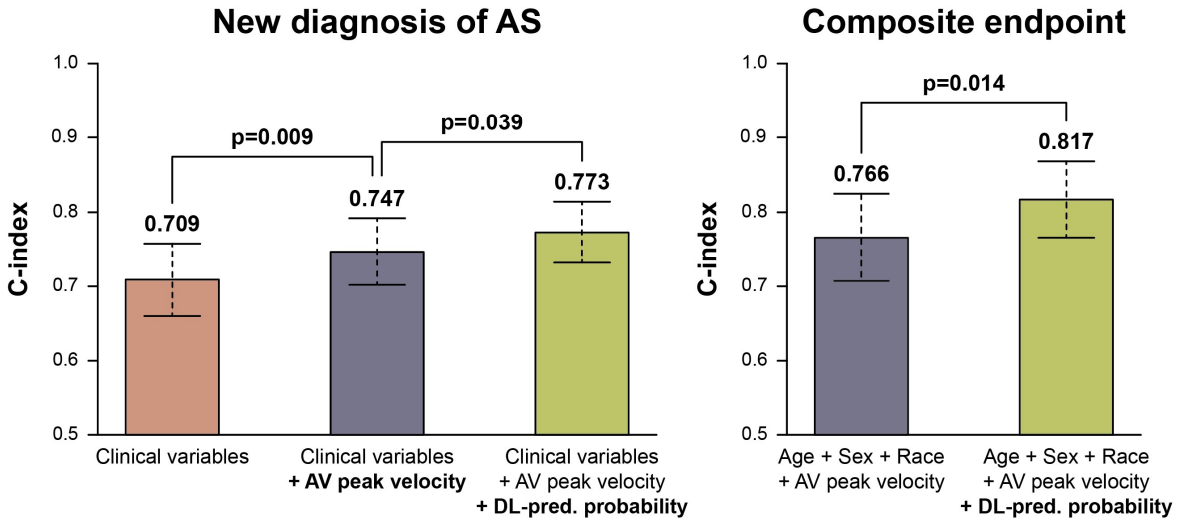

Figure 4 Sequential Cox regression models for predicting the new diagnosis of AS and the composite endpoint in patients with AV sclerosis in the ARIC cohort

Clinical variables include age, sex, race, hypertension, diabetes, history of heart failure, history of coronary heart disease, and history of atrial fibrillation.

Abbreviations as in Figures 1 and 2.

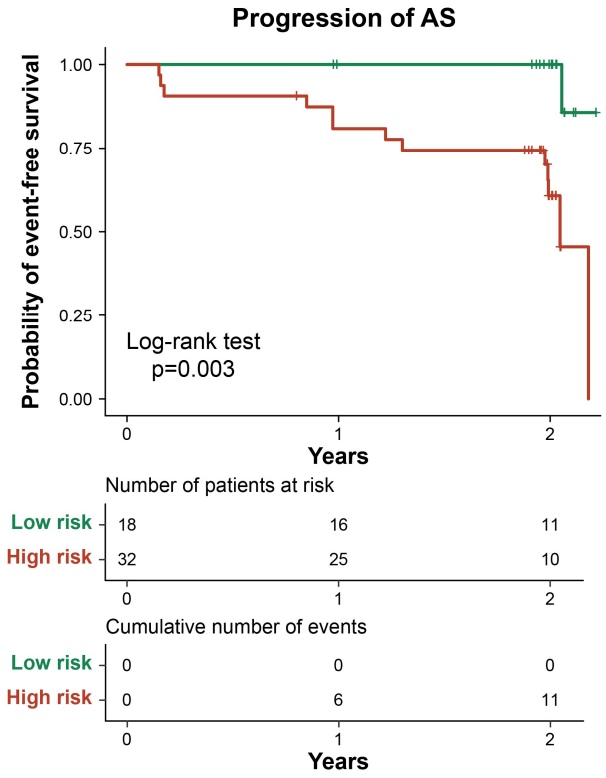

Figure 5 Kaplan-Meier curves showing the event-free survival of patients in the CMR cohort

The cut-off value optimized in the ARIC cohort (i.e., the DD probability value of 0.81) was used to stratify patients into low-risk and high-risk groups.

CMR – cardiac magnetic resonance; other abbreviations as in Figure 1.

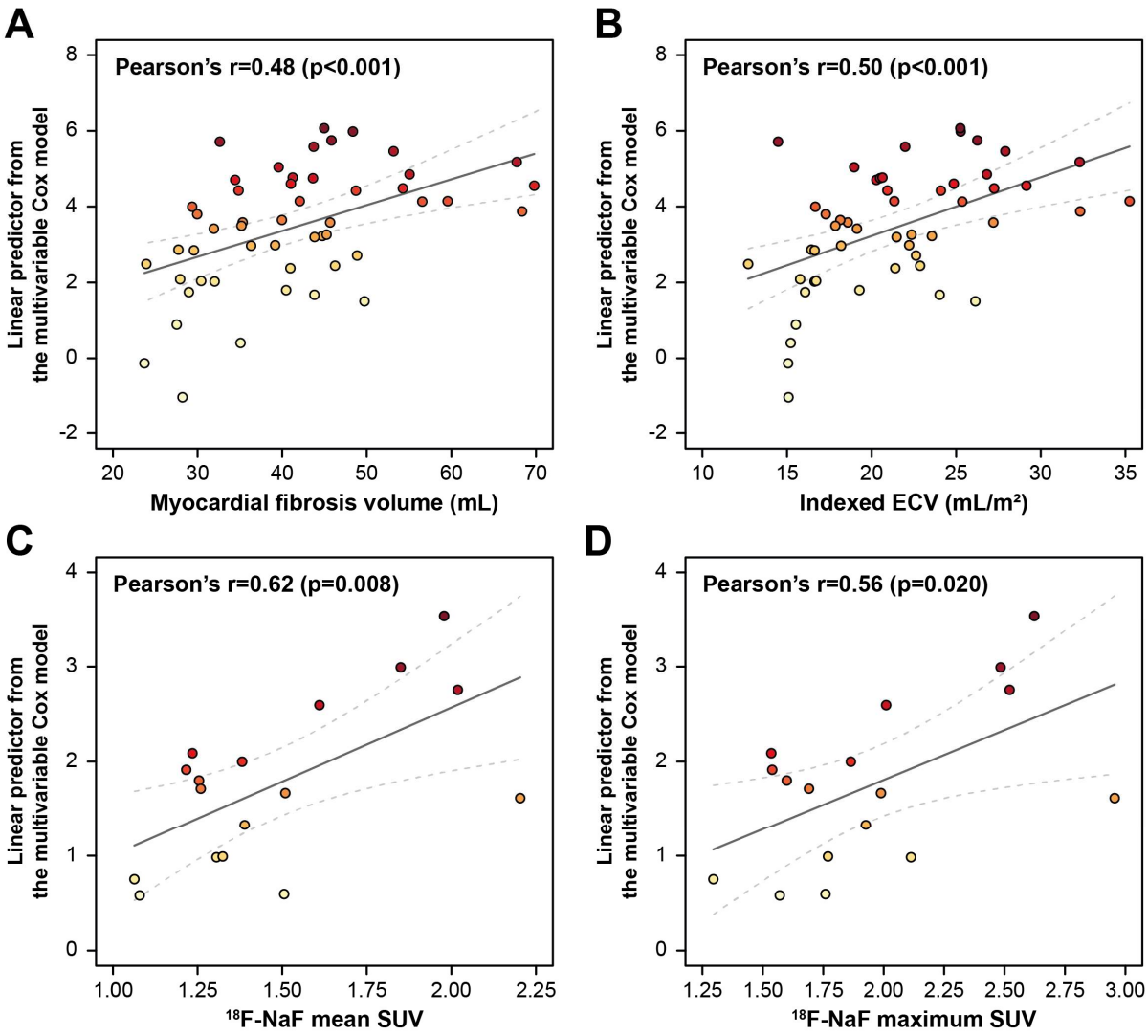

Figure 6 Correlations between the linear predictor calculated based on the multivariable Cox model and LGE-based myocardial fibrosis volume (A), indexed ECV assessed using myocardial T1 mapping (B), and valvular ^{18}F-NaF uptake quantified using PET/CT (C and D)
^{18}F-NaF – ^{18}F-sodium fluoride, ECV – extracellular volume, LGE – late gadolinium enhancement, PET/CT – positron emission tomography combined with computed tomography, SUV – standardized uptake value

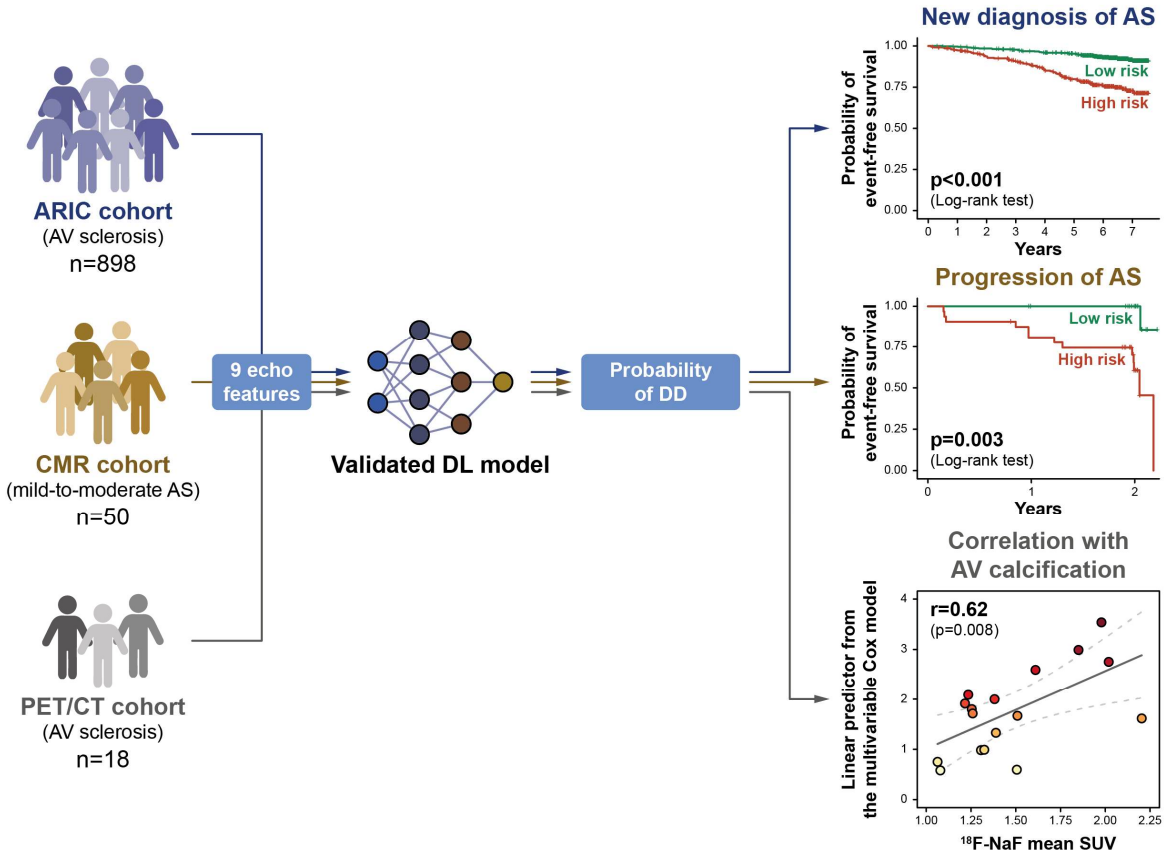

Central Illustration Associations between the DL-predicted DD and the development and progression of AS in patients with early-stage AV disease

In this study, we investigated whether a previously validated echocardiography-based DL model assessing DD could identify the latent risk associated with the progression of early-stage AS. In participants with AV sclerosis from the ARIC cohort study, we determined the optimal DD probability threshold (0.81) for identifying individuals with high and low risk of progressing from AV sclerosis to AS. This threshold was subsequently used in an external cohort of patients with mild-to-moderate AS who underwent CMR imaging at baseline and annual echocardiographic assessments for two consecutive years. We found that high-risk patients (DD probability ≥0.81) had larger indexed extracellular volumes on CMR at baseline and were more likely to exhibit a progression in AS during follow-up than those classified into the low-risk group (DD probability <0.81). Last, in a third cohort with AV sclerosis undergoing PET/CT, the linear predictor calculated using the multivariable Cox model incorporating the

DL-predicted probability of DD correlated positively with valvular ^{18}F-NaF uptake, confirming that the latent risk identified by the model is associated with the underlying milieu of valvular inflammation and calcification.

Abbreviations as in Figures 1, 2, 5, and 6.